Supporting Information for:

Supramolecular Chiral Self-Assembly and Supercoiling Behavior of Carrageenans at Varying Salt Conditions

Larissa Schefer, Jozef Adamcik, Michael Diener and Raffaele Mezzenga*

Department of Health Sciences and Technology, ETH Zurich, Schmelzbergstrasse 9, 8092 Zurich, Switzerland

* E-mail: raffaele.mezzenga@hest.ethz.ch

Experimental Section

Materials

Kappa (22048, CAS 11114-20-8, LOT# BCBF0535V) and iota carrageenan (C4014, type V, CAS 9062-07-1, LOT# 066K1725V) were obtained from Sigma-Aldrich. Ultrapure water (18.2 MΩ·cm at 25 °C) was obtained from a MilliQ integral water purification system (Millipore Corporation). Sodium chloride (NaCl for analysis, EMSURE, CAS 7647-14-5, ≥ 99.5%) and calcium chloride ($CaCl_2$*2 H_2O for analysis, EMSURE, CAS 10035-04-8, 99-102%) were purchased from Merck, whereas potassium chloride (KCl, CAS Registry No. 7447-40-7, puriss 99-100.5%) and (3-Aminopropyl)triethoxysilane (APTES, CAS 919-30-2, 99%) for mica modification were obtained from Sigma-Aldrich. Dialysis membranes (7 Spectra/Por® standard grade dialysis tubing, regenerated cellulose, 50 kDa MWCO) used for carrageenan purification were purchased from Spectrum Laboratories.

Sample Preparation and Purification

Commercially obtained kappa and iota carrageenan were individually dissolved in MilliQ water to yield stock solutions of 0.05% w/w, which were left to rest overnight at room temperature to achieve complete dissolution. Stock solutions were then purified at room temperature by dialysis against MilliQ water to remove excess salts (bath changes after 2, 4, and 8 h), transformed into the Na-, K- and Ca-form by ion-exchange against NaCl, KCl and $CaCl_2$ (bath changes after 24, 26, 28, and 32 h), before being again subjected to another dialysis step against MilliQ to remove any excess salts introduced by ion-exchange (bath changes after 48, 50, 52, and 56 h; stop of purification after 72 h). The ionic composition in terms of Na, K, and Ca was analyzed by Flame Atomic Absorption Spectrophotometry to confirm the effectivity of the purification protocol (Table S1). The concentration of the purified carrageenan samples was checked by Optical Rotatory Dispersion (ORD) based on a linear regression of carrageenan calibration samples of known concentration and was used for the dilution calculation to prepare samples with polymer concentrations of 1 µg/mL for standard AFM and 50 µg/mL for PF-QNM experiments.

To obtain carrageenan solutions containing NaCl, KCl or $CaCl_2$, respectively, the purified solutions were first diluted with MilliQ water, turned upside down several times to achieve homogenous distribution, and the volume of saline solution required to yield added salt concentrations varying from 0 to 150 mM NaCl, KCl or $CaCl_2$ was then added and again turned upside down before deposition for AFM imaging. For KCl, which was found to trigger the formation of superstructures, also higher added salt concentrations of 250, 500, 750, and 1000 mM KCl were examined.

Apparatus and Techniques

Flame Atomic Absorption Spectrophotometry. Calibration and carrageenan samples were prepared in tubes pretreated with HNO_3 by using KNO_3 as a matrix modifier for Na- and Ca-determination, or $CsNO_3$ for the determination of K. The measurements were performed in an air/acetylene flame on a 240FS AA fast sequential atomic absorption spectrometer (Agilent technologies) at 589.0 nm for Na and 766.5 nm for K. Ca was measured in a N_2O/acetylene flame at 422.7 nm. The ionic compositions of purified kappa and iota carrageenan in the Na-, K- and Ca-form, respectively, are summarized in Table S1.

Table S1. Ionic compositions of kappa, iota, and lambda carrageenan after transformation to the K- and Ca-form by combining dialysis and ion-exchange, as determined by Flame Atomic Absorption Spectrophotometry.

carrageenan	Na^+ [wt%]	K^+ [wt%]	Ca^{2+} [wt%]
kappa-Na	3.248	0.001	0.110
iota-Na	6.709	0.004	0.546
kappa-K	< detection	5.461	0.089
iota-K	< detection	13.145	0.558
kappa-Ca	< detection	< detection	3.698
iota-Ca	< detection	< detection	4.739

Optical Rotatory Dispersion (ORD). The measurements of calibration samples and carrageenan solutions after purification were performed on a J-815-150S CD spectrometer with an ORDE-402/15 accessory (Jasco Inc.). Sample aliquots of 1.5 mL were transferred into a cylindrical glass cell with a path length of 100 mm (Jasco Parts Center). ORD and high tension signals were then recorded with standard sensitivity in two accumulations at ambient temperature from 600 to 300 nm, with a data pitch of 0.2 nm, a scanning speed of 100 nm/min, a digital integration time of 1 s, and a band width of 5 nm. The calibration curve was obtained from the linear regression of ORD values at 350 nm.

Atomic Force Microscopy (AFM). For AFM imaging, the mica surface was treated with APTES to obtain a positively charged mica substrate (AP-mica), which allows an effective immobilisation of the negatively charged carrageenan polymers[1], which follow a 2D equilibrated worm-like chain behavior as confirmed by a previous excess kurtosis analysis[2]. Briefly, a freshly prepared 0.05% v/v aqueous APTES solution was incubated on a cleaved mica surface for 1 min, thoroughly rinsed with 3 mL MilliQ water, and dried with pressurized air. Sample aliquots of 20 µL were deposited onto the AP-mica substrate, left to adsorb for 30 s at room temperature, rinsed drop-wise with 1 mL MilliQ water, and gently dried with pressurized air.

The surface topologies of samples in dry-state were scanned on Nanoscope VIII Multimode Scanning Force Microscopes and a Dimension FastScan Bio (both from Bruker AXS) covered with an acoustic hood to minimize vibrational noise. The AFMs were operated in tapping mode under ambient conditions using commercial silicon nitride cantilevers. AFM images were acquired continuously with a lateral resolution of at least 0.5 pixels per nm for normal resolution (Figure 1 and Figures S1-S4), 0.7 pixels per nm for super high resolution (Figures 2 and 3 and Figures S5-S8 and S10-S12 and S14-S19), and 1.7 pixels per nm for images used for estimation of periodic height fluctuations (Figure 2(e) and Figure S9). All AFM images were flattened to remove background curvature using the Bruker NanoScope Analysis 1.5 software and no further image processing was carried out.

The cross sectional analyses (Figures 2(a, c, d, g) and 3(a, c)) were done and extracted from the Bruker NanoScope Analysis 1.5 software, whereas height profiles along the polymer or superstrand contours (Figures 2(e), 3(e), S9(c, e), and S18(d)) and periodicity analyses with pitch size estimations based on discrete Fourier transform (DFT) function of the height profiles (Figures S10(d, f) and S17(e)) were done by using the specially designed and open-source software "FiberApp"[3].

AFM Peak Force Quantitative Nanomechanical (PF-QNM) Technique. For PF-QNM measurements of the superstrands of kappa carrageenan (50 µg/mL) in presence of 100 mM KCl, besides following the AFM sample preparation as described above (Figure S13(b)), a modified protocol to form a thick film (Figure S13(a)) was applied. For the latter, a sample aliquot of 50 µL was deposited onto the AP-mica substrate and left drying for 2 h at ambient conditions while the sample was covered with a petri dish to prevent any contamination. PF-QNM experiments were performed on a Nanoscope VIII Multimode Scanning Force Microscope. The experiment was done in liquid by flushing the sample cell with 100 mM KCl and by using ScanAsyst Fluid cantilevers (Bruker) which were calibrated before measurements. The analysis of the Derjaguin–Mueller–Toporov (DMT) modulus was performed by using the Bruker NanoScope Analysis 1.5 software.

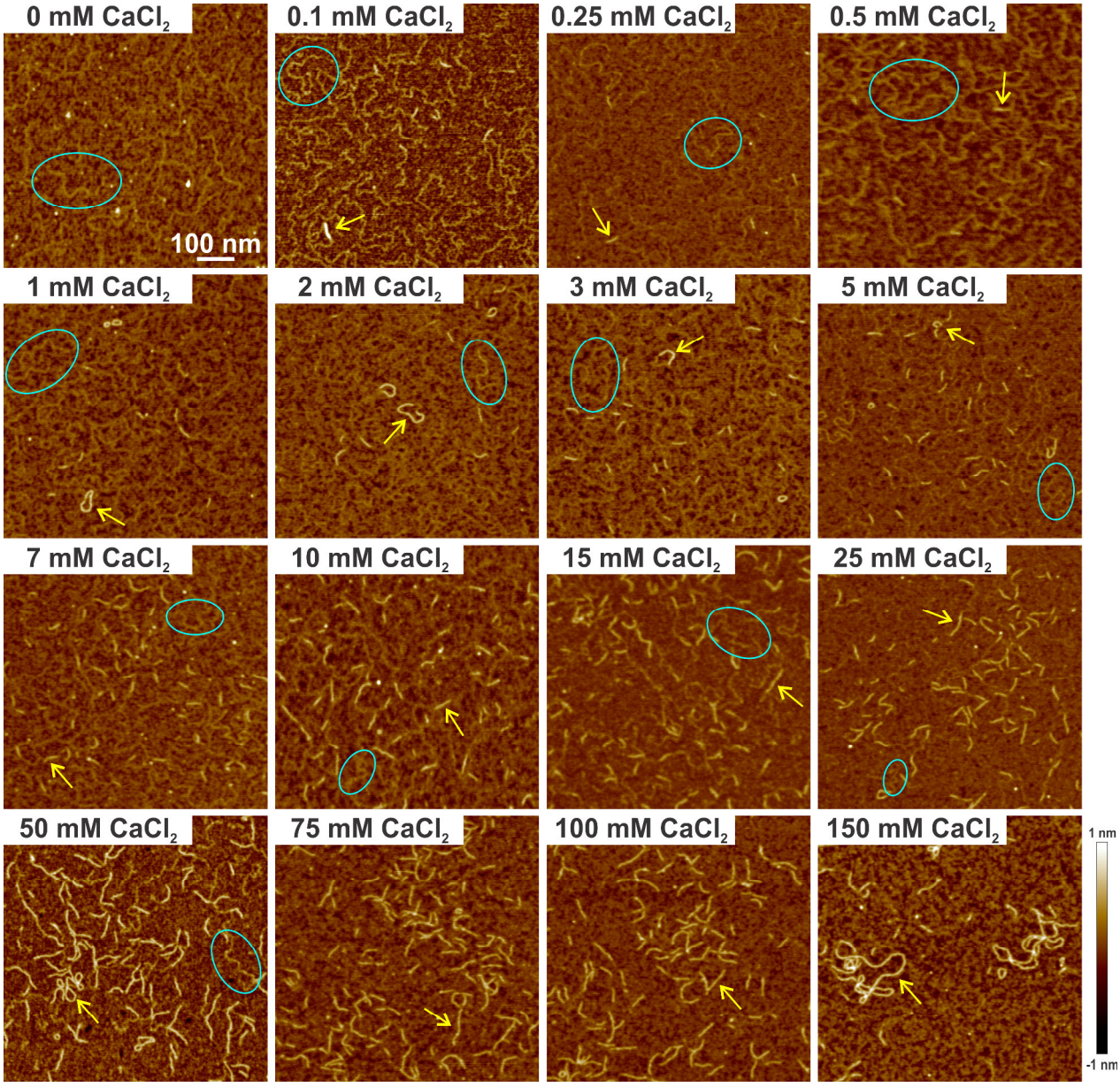

Figure S1. AFM height images of kappa carrageenan (1 µg/mL) in presence of 0, 0.1, 0.25, 0.5, 1, 2, 3, 5, 7, 10, 15, 25, 50, 75, 100 and 150 mM added $CaCl_2$ reveal a progressive transition of flexible random coils (indicated by blue ellipses) to rather stiff single helices (indicated by yellow arrows), which do not indicate any further supramolecular self-assembly process. The scale and color bars apply to all AFM images.

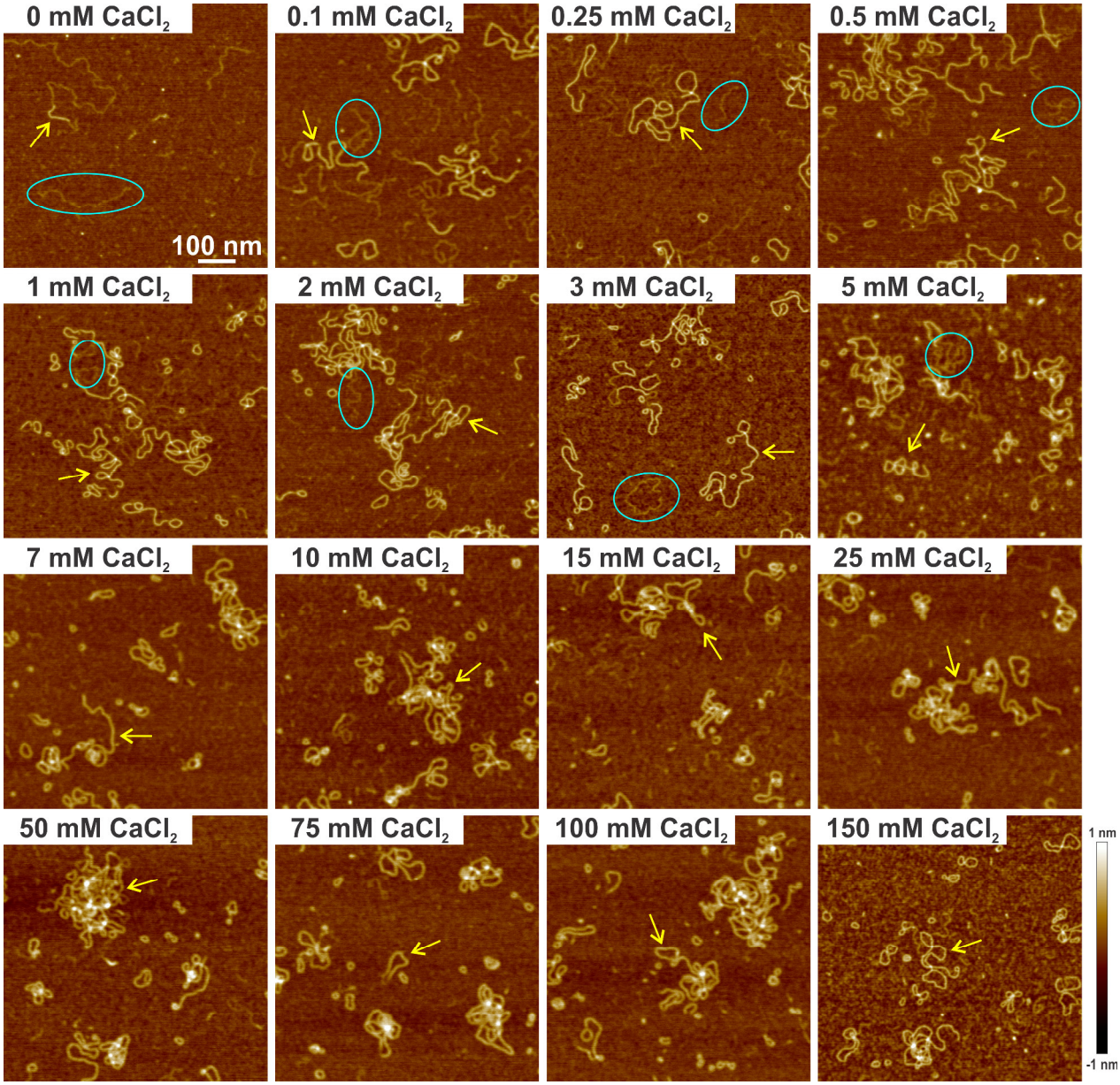

Figure S2. AFM height images of iota carrageenan (1 µg/mL) in presence of 0, 0.1, 0.25, 0.5, 1, 2, 3, 5, 7, 10, 15, 25, 50, 75, 100 and 150 mM added $CaCl_2$ reveal a progressive transition of flexible random coils (indicated by blue ellipses) to stiffer single helical conformations (indicated by yellow arrows) which cluster akin to the condensation process as observed for DNA[4]. The scale and color bars apply to all AFM images.

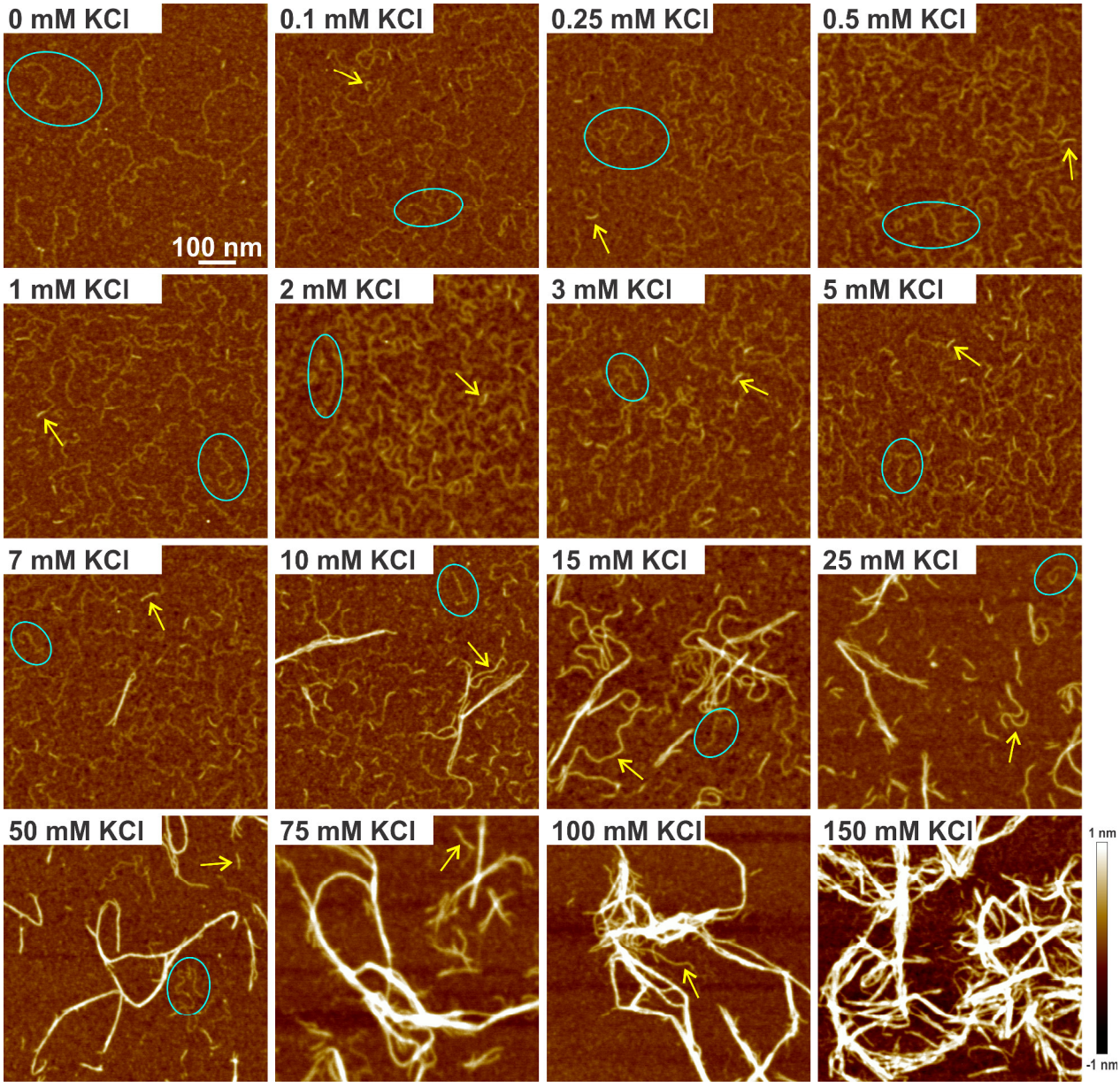

Figure S3. AFM height images of kappa carrageenan (1 µg/mL) in presence of 0, 0.1, 0.25, 0.5, 1, 2, 3, 5, 7, 10, 15, 25, 50, 75, 100 and 150 mM added KCl reveal a progressive transition of flexible random coils (indicated by blue ellipses) to rather stiff single helices (indicated by yellow arrows), which, via transient states form strands which further aggregate to superstrands and crosslink while forming a network. The scale and color bars apply to all AFM images.

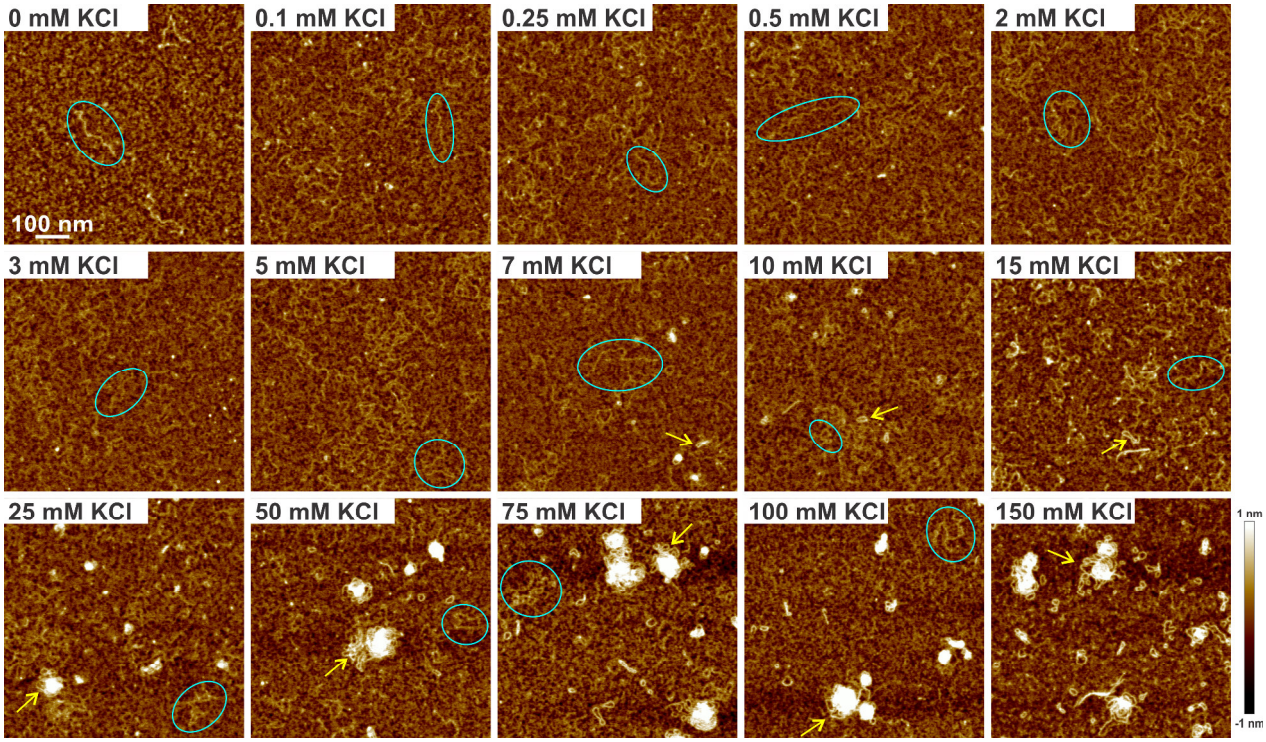

Figure S4. AFM height images of iota carrageenan (1 µg/mL) in presence of 0, 0.1, 0.25, 0.5, 2, 3, 5, 7, 10, 15, 25, 50, 75, 100 and 150 mM added KCl reveal a coil-helix transition with a concurrent clustering to flower-shaped aggregates akin to morphologies observed with DNA[5] before. Selected random coils are indicated by blue ellipses, whereas yellow arrows indicate chains in single helical conformation. The scale and color bars apply to all AFM images.

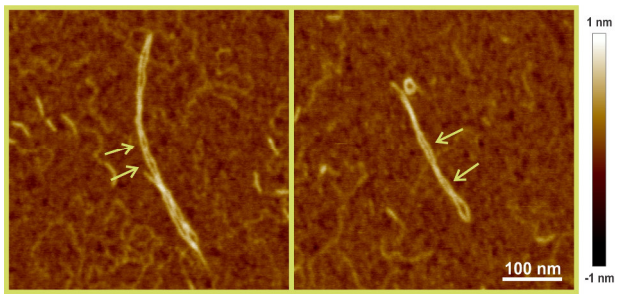

Figure S5. AFM height images of kappa carrageenan (1 µg/mL) in presence of 7 mM added KCl revealing the onset of twisting of carrageenan strands in helical conformation. The splitting polymer chain ends (left image) indicate an intermolecular dimerization process of two individual single helical polymer chains, whereas bubble or hairpin-loop[6] morphologies (right image) at one of the strand ends point towards an intramolecular process of a single helical polymer chain. The scale and color bars apply to all AFM images.

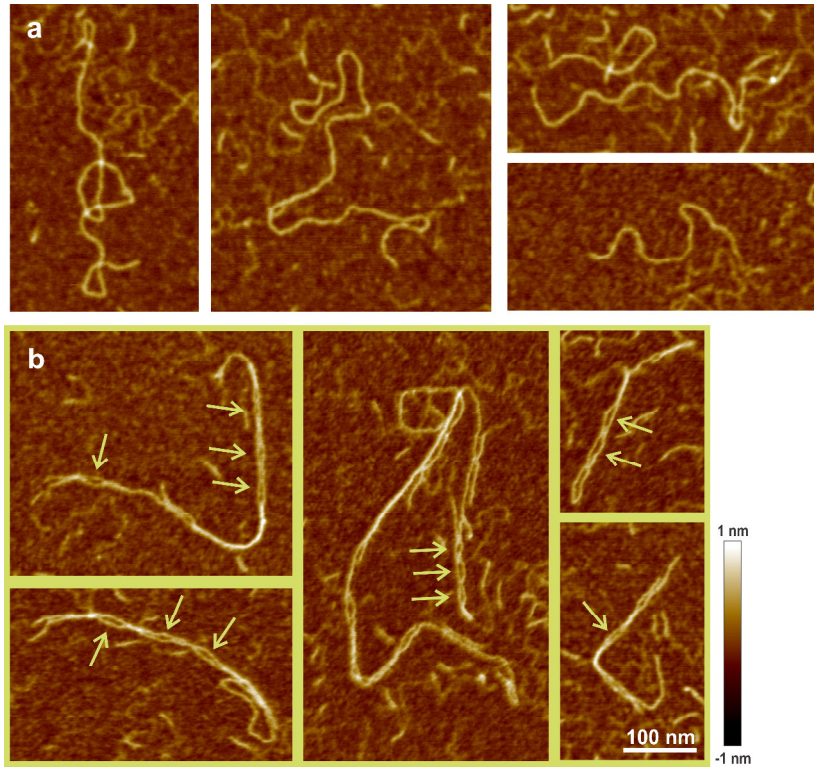

Figure S6. AFM height images of kappa carrageenan (1 µg/mL) in presence of 10 mM added KCl with coexisting (a) non-interacting carrageenan polymers in single helical conformation and (b) inter- and intramolecular (top right image shows a hairpin-loop[6] morphology) loose twisting of the helical strands (arrows indicate bubbles as a result of the loose twisting). The scale and color bars apply to all AFM images.

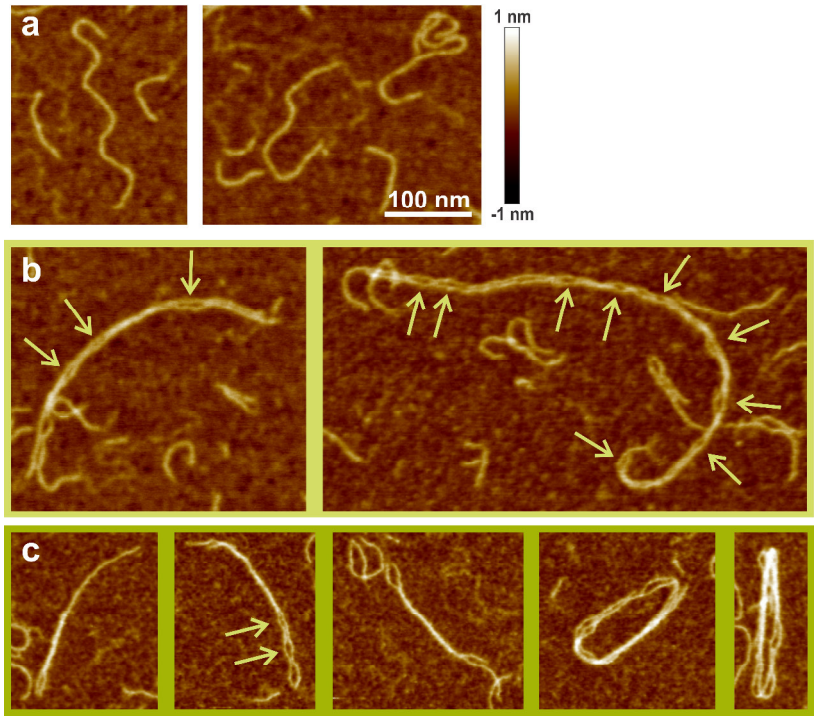

Figure S7. AFM height images of kappa carrageenan (1 µg/mL) in presence of 15 mM added KCl where the vast majority of polymer chain underwent the coil-helix transition with coexisting (a) non-interacting, (b) intermolecular loose twisted (arrows indicate bubbles) and (c) inter- and intramolecular tight intertwined helical polymer strands. The scale and color bars apply to all AFM images.

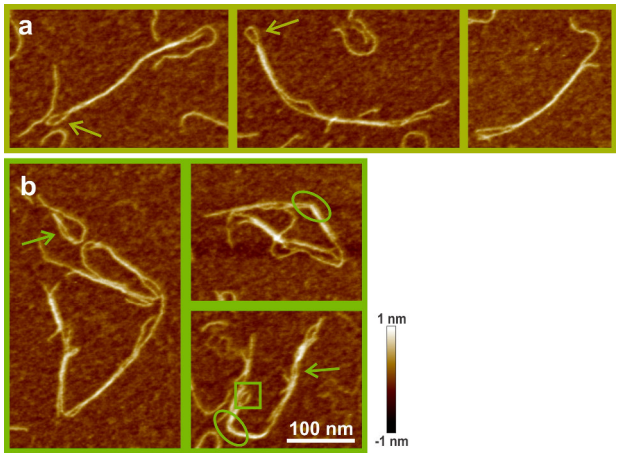

Figure S8. AFM height images of kappa carrageenan (1 µg/mL) in presence of 25 mM added KCl with coexisting (a) tight intertwined helical polymer strands with bubble and hairpin-loop[6] structural features (indicated by arrows) and (b) multi-filament (frayed ends indicated with a square) structures featuring kinks (indicated with ellipses). The scale and color bars apply to all AFM images.

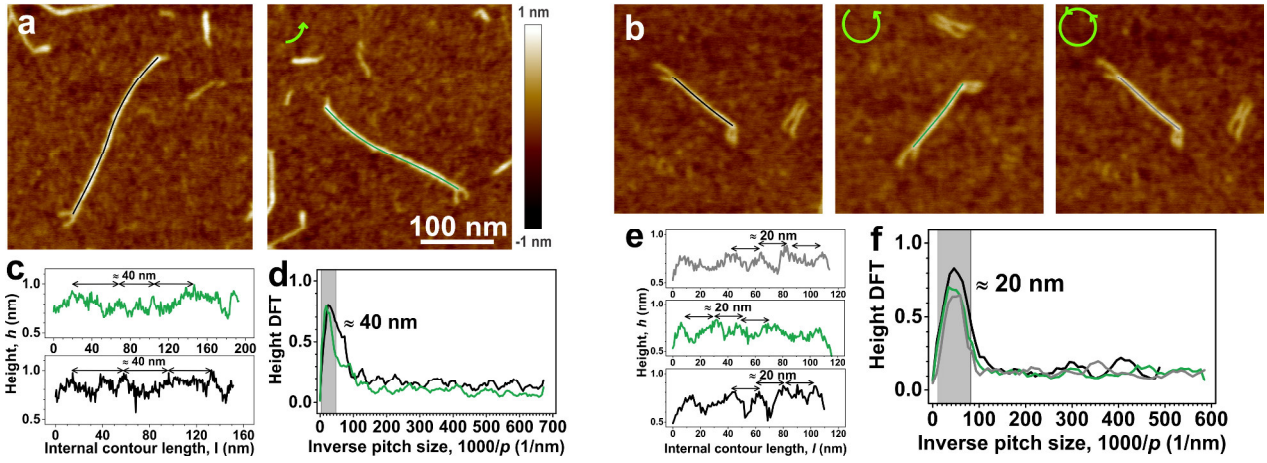

Figure S9. (a, b) AFM height images of kappa carrageenan tight intertwined helical strands in presence of 50 mM added KCl obtained at different AFM scanning angles of (a) 0 or 90° and (b) 0, 270 or 360° (indicated with the green arrows). (c-f) The periodic height fluctuations along the intertwined fibril contours and the corresponding pitch size estimations based on discrete Fourier transform (DFT) function of the height profiles of about (c, d) 40 and (e, f) 20 nm appear independent of the AFM scanning angle. The scale and color bars apply to all AFM images.

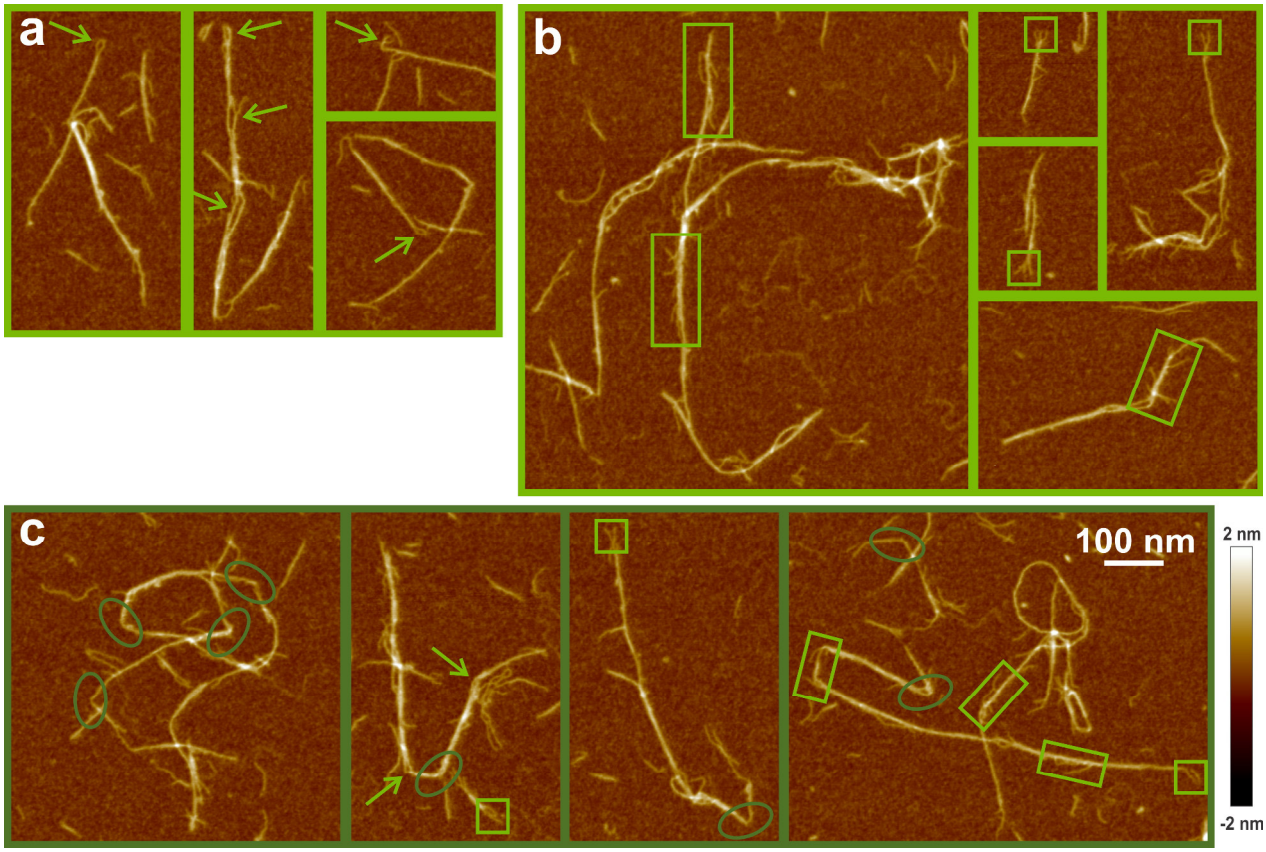

Figure S10. AFM height images of kappa carrageenan (1 µg/mL) in presence of 50 mM added KCl showing coexisting (a) loose twisted and tight intertwined fibrils with bubbles (indicated with arrows), (b) frayed ends (indicated with squares) suggesting multi-filament hierarchical structure, and (c) superstructures combining the characteristic features of bubbles, hairpin-loops[6], frayed ends and kinks (indicated with ellipses). The scale and color bars apply to all AFM images.

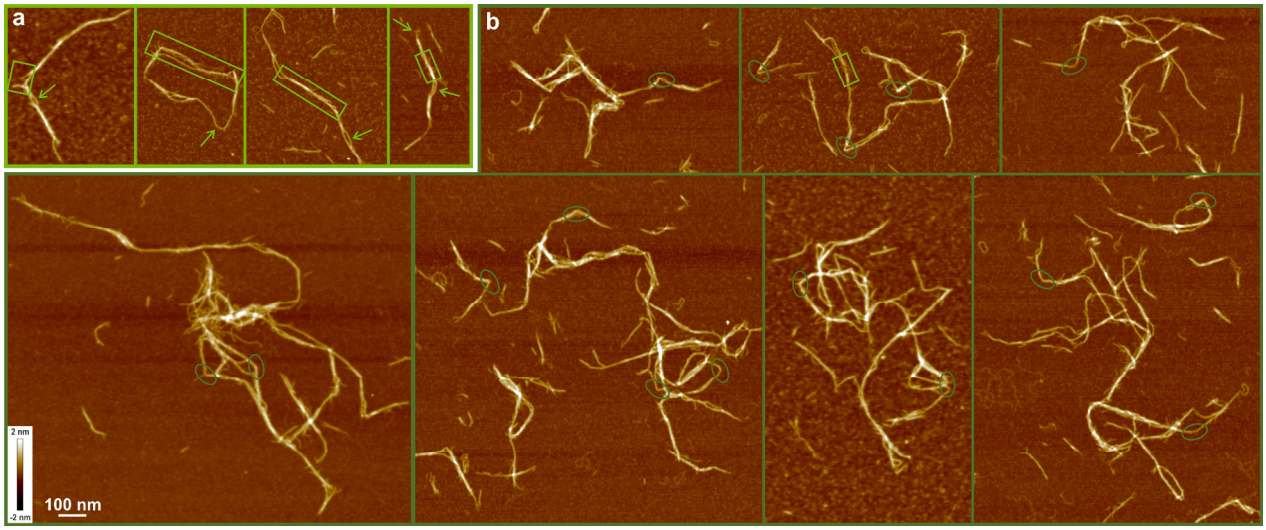

Figure S11. AFM height images of kappa carrageenan (1 µg/mL) in presence of 100 mM added KCl with detailed structural features of (a) bubbles (indicated by arrows) and frayed ends indicating the formation of multi-filament fibrils and (c) superstructures with kink formation (indicated with ellipses) and frayed ends (indicated with squares). The scale and color bars apply to all AFM images.

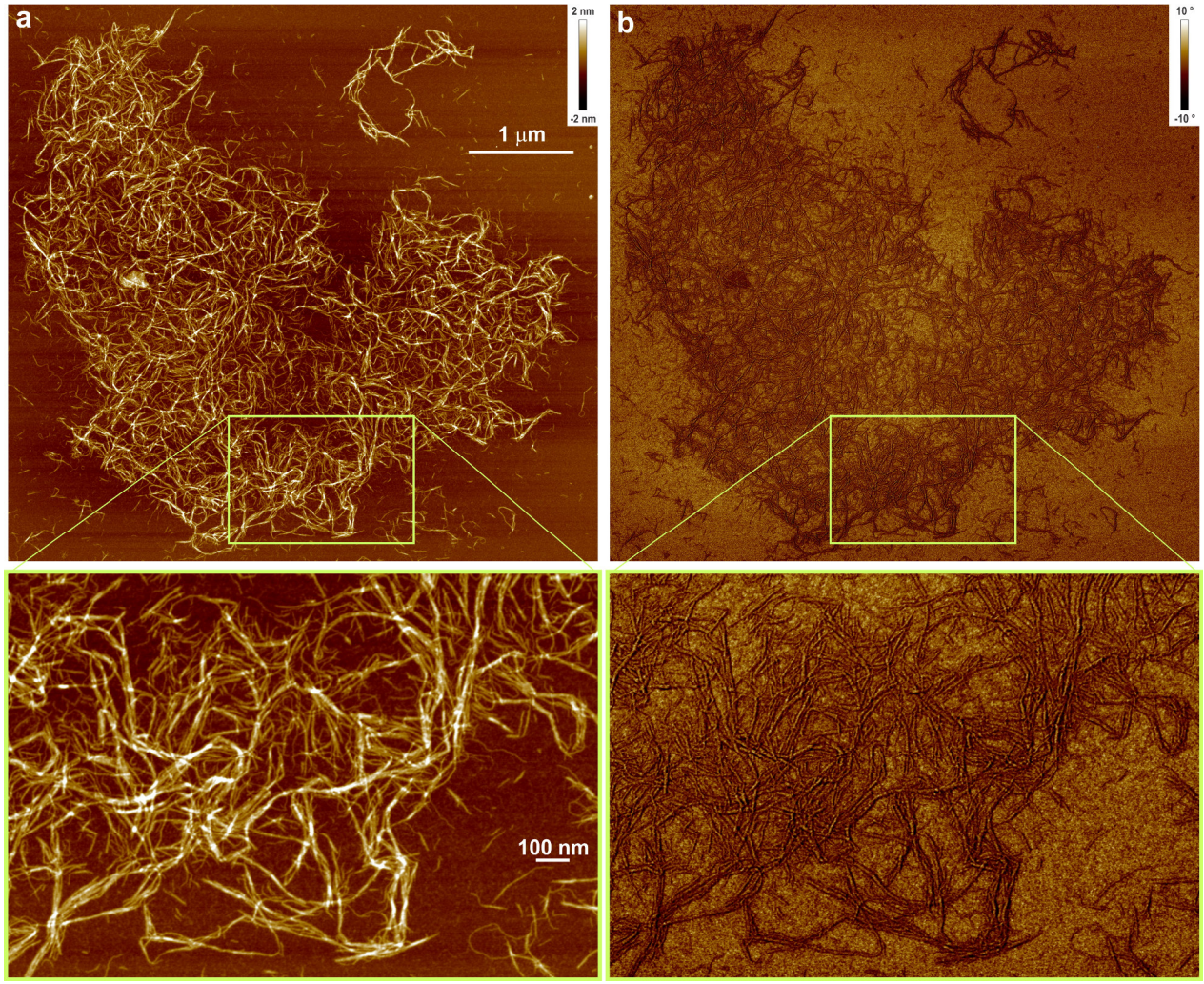

Figure S12. AFM height (a) and corresponding phase (b) images of kappa carrageenan (1 µg/mL) in presence of 150 mM added KCl where superstructures aggregate into complex networks. The scale and color bars apply to all AFM images.

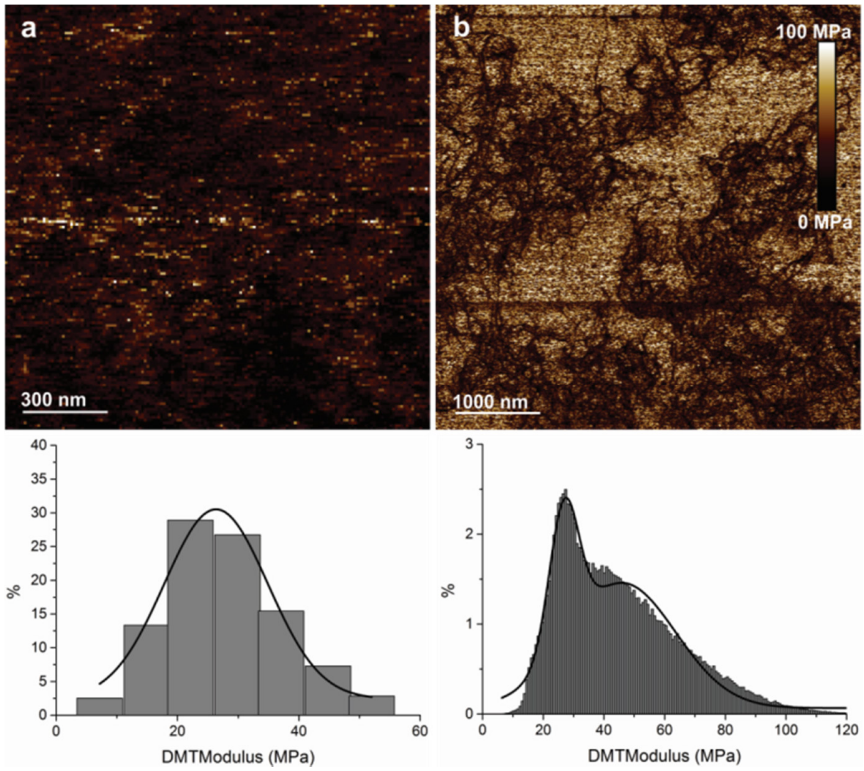

Figure S13. AFM DMT modulus images of kappa carrageenan (50 µg/mL) in presence of 100 mM KCl on (a) a thick film (modified sample preparation protocol) and (b) a network of superstructures (standard AFM sample preparation) with the corresponding DMT modulus distributions. The superstructure network yields a bimodal DMT modulus distribution with a peak at around 26 MPa in line with the peak observed for the thick film.

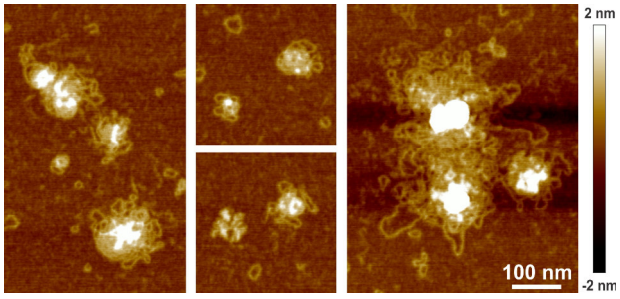

Figure S14. AFM height images of iota carrageenan (1 µg/mL) in presence of 150 mM added KCl appearing as flower-shaped clusters with single helical carrageenan loops emerging from a dense core, a morphological feature which was previously described for DNA[5]. The scale and color bars apply to all AFM images.

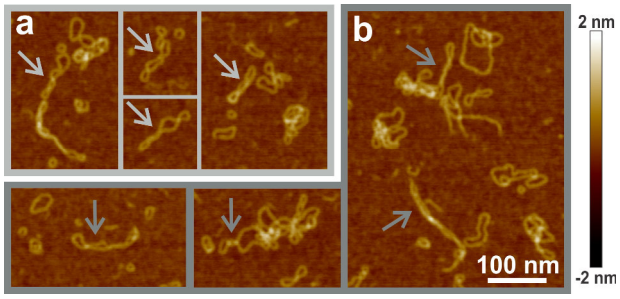

Figure S15. AFM height images of supercoiling iota carrageenan (1 µg/mL) in presence of 250 mM added KCl showing (a) loose twisting and (b) tight intertwining of the helical polymer strands. This supercoiling behavior resembles the morphological details previously described for DNA[7] and schizophyllan polysaccharide[8], respectively. The scale and color bars apply to all AFM images.

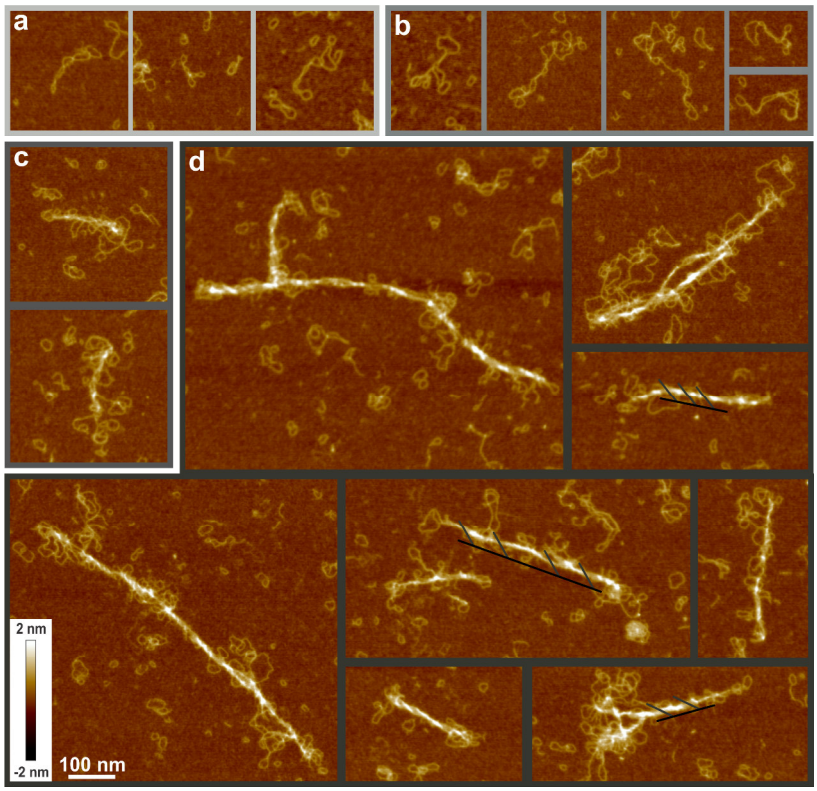

Figure S16. AFM height images of supercoiling iota carrageenan (1 µg/mL) in presence of 500 mM added KCl with coexisting (a) loose twisted and (b) tight intertwined helical strands, akin to previously described DNA[7] and schizophyllan[8] morphologies, respectively, further assembling into (c) intermediate pre-structures and (d) mature supramolecular hierarchical structures which in certain cases unveil periodic height fluctuations and a right-handed helical twist as marked by the tilt angles. The scale and color bars apply to all AFM images.

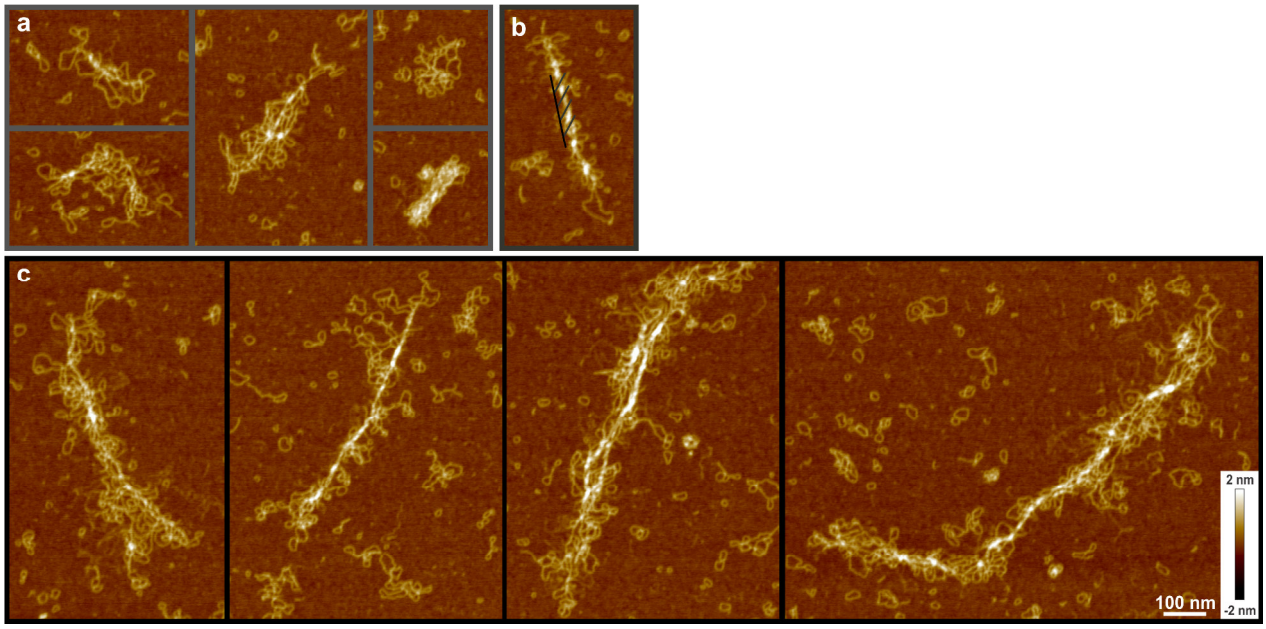

Figure S17. AFM height images of iota carrageenan (1 µg/mL) in presence of 750 mM added KCl with coexisting (a) self-assembled intermediate pre-structures, (b) supramolecular chiral structures and (c) lateral widening of superstructures. The scale and color bars apply to all AFM images.

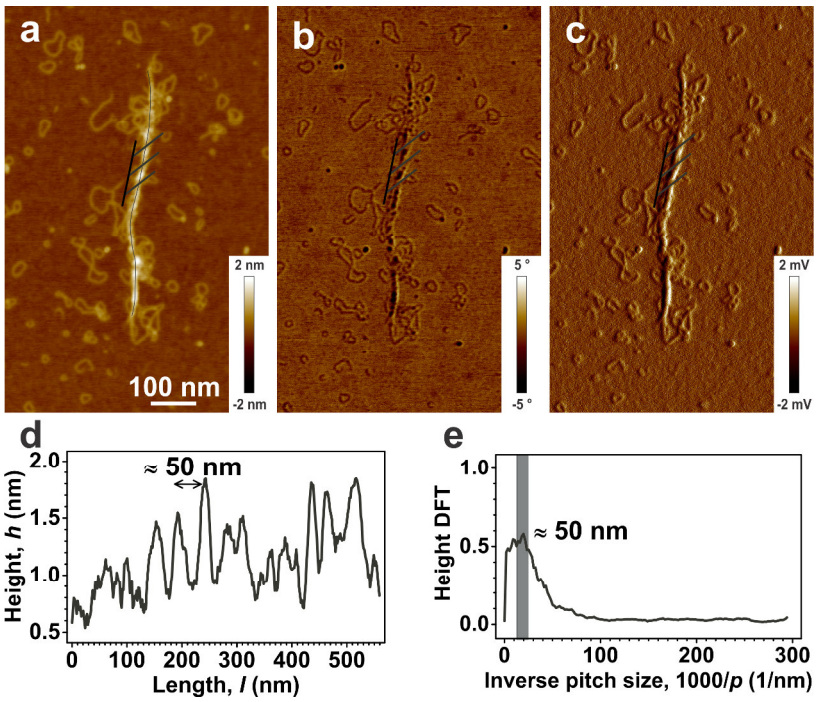

Figure S18. AFM (a) height and corresponding (b) phase and (c) amplitude images of a characteristic supramolecular chiral iota carrageenan structure with a periodic height fluctuations and a right handed helical twist as marked by the tilt angle, obtained in presence of 500 mM added KCl. The scale and color bars apply to all AFM images. (d) The height profile along the superstrand contour and (e) the corresponding pitch size estimation based on discrete Fourier transform (DFT) function, both reveal a pitch of 50 nm.

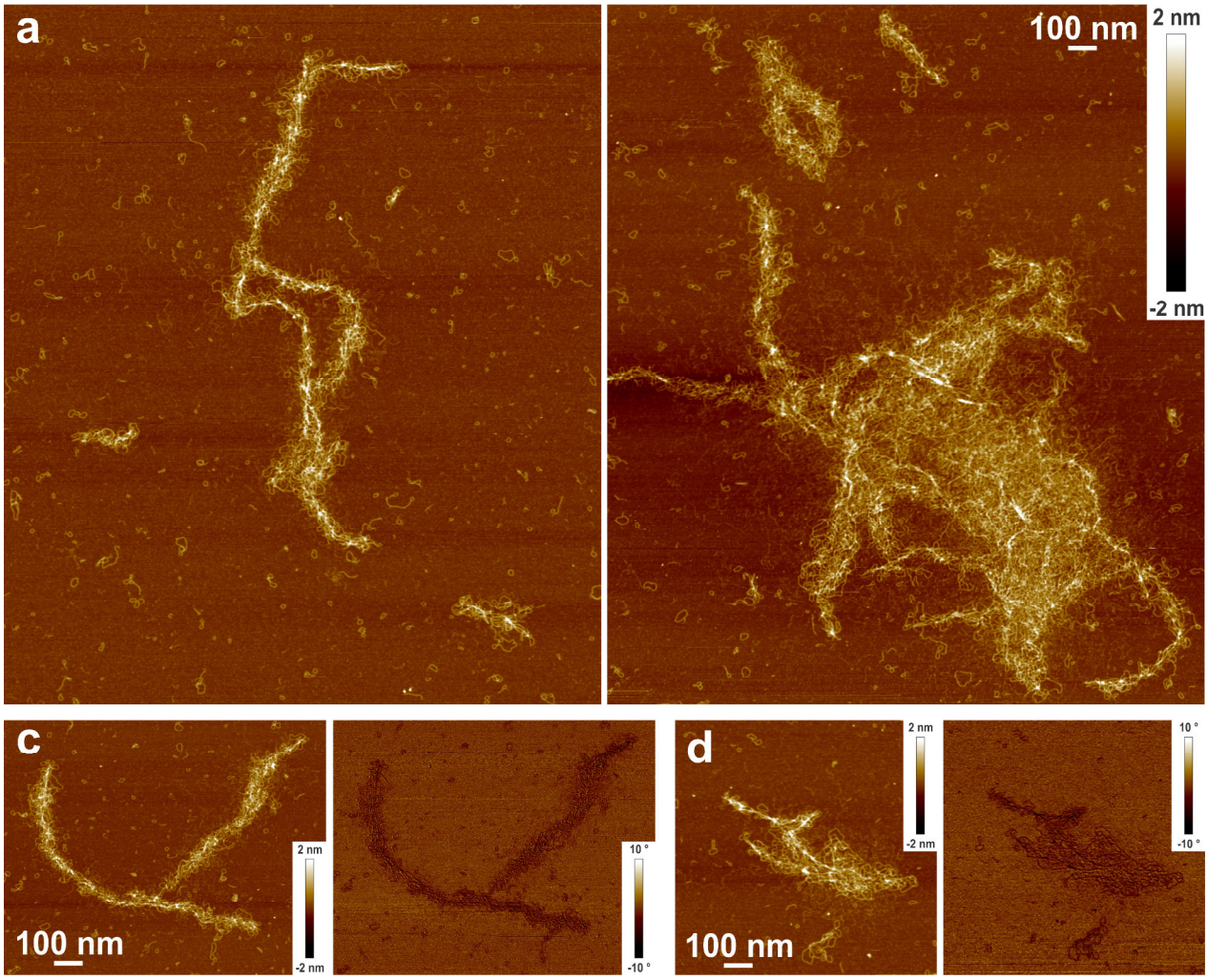

Figure S19. AFM (a-c) height and (c,d) corresponding phase images of iota carrageenan (1 µg/mL) in presence of 1000 mM added KCl showing aggregated supramolecular superstructures forming a network of several microns in diameter. The scale and color bars apply to all AFM images.

References

1 L. Schefer, J. Adamcik and R. Mezzenga, *Angew. Chem. Int. Ed.*, 2014, **53**, 5376.
2 L. Schefer, I. Usov and R. Mezzenga, *Biomacromolecules*, 2015, **16**, 985.
3 I. Usov and R. Mezzenga, *Macromolecules*, 2015, **48**, 1269.
4 L. R. Brewer, R. Friddle, A. Noy, E. Baldwin, S. S. Martin, M. Corzett, R. Balhorn and R. J. Baskin, *Biophys. J.*, 2003, **85**, 2519.
5 (a) Y. Fang and J. H. Hoh, *J. Am. Chem. Soc.*, 1998, **120**, 8903; (b) F. Sansone, M. Dudič, G. Donofrio, C. Rivetti, L. Baldini, A. Casnati, S. Cellai and R. Ungaro, *J. Am. Chem. Soc.*, 2006, **128**, 14528.
6 (a) R. M. Abeysekera, E. T. Bergström, D. M. Goodall, I. T. Norton and A. W. Robards, *Carbohydr. Res.*, 1993, **248**, 225; (b) Y.-F. Wei and P.-Y. Hsiao, *J. Chem. Phys.*, 2007, **127**, 064901.
7 (a) Y. L. Lyubchenko and L. S. Shlyakhtenko, *Proc. Natl. Acad. Sci. USA*, 1997, **94**, 496; (b) L. S. Shlyakhtenko, L. Miloseska, V. N. Potaman, R. R. Sinden and Y. L. Lyubchenko, *Ultramicroscopy*, 2003, **97**, 263.
8 B. T. Stokke, A. Elgsaeter, D. A. Brant and S. Kitamura, *Macromolecules*, 1991, **24**, 6349.